AUTOMATYKA • 2011 • Tom 15 • Zeszyt 3

Tomasz Węgliński*, Anna Fabijańska*

Image Segmentation Algorithms for Diagnosis Support of Hydrocephalus in Children

1. Introduction

Radiology is one of the most rapidly developing fields of medicine. It plays an important role in the modern clinical treatment. With the growing popularity of medical imaging techniques, many diseases can be detected at the early stage of their progress. Furthermore, imaging examinations help in the decision to open surgery and are used in the postoperative control of the patient.

There are several radiological examinations used for the imaging of different areas of human body. Most popular techniques include computed tomography (CT), magnetic resonance imaging (MRI), positron emission tomography (PET) and ultrasonography (USG). These methods are widely used in the diagnosis of lesions within human abdomen, heart, lung, brain etc.

In this paper attention is focused on CT investigation of one of the most serious brain dysfunction called hydrocephalus.

Hydrocephalus (also known as "water on the brain") is the pathology most commonly affecting newborns, but it can also arise due to other abnormalities in the functioning of the brain. The disease is complex, hence there is no clearly established and accepted definition of hydrocephalus. In most studies the definition of this lesion is usually replaced by its descriptive characteristics which draws attention to the presence of three following symptoms [1]:

- increase of intracranial pressure,
- increase the volume of cerebrospinal fluid (CSF),
- expansion of the intracranial fluid spaces.

The only way to deal with hydrocephalus is surgical treatment [2]. However, not every ventricular enlargement of brain is caused by hydrocephalus and requires surgery. For this reason, precise assessment and diagnosis of hydrocephalus is an important step in treatment

* Computer Engineering Department, Technical University of Lodz, Poland

planning. Recently, the assessment of pathological changes due to hydrocephalus is based on CT or MRI brain scans. However, such assessment is still performed manually or semi-manually by a radiologist. Automation of this process may increase efficiency of lesion detection and eliminate the problem of subjective assessment of the disease.

The presented research considers the problem of an automatic detection of hydrocephalus in CT images. For this purpose, several thresholding algorithms were tested and compared with the proposed, new method for segmentation based on seeded region growing. The results of this comparison were presented and discussed.

2. Related works

Recent studies of hydrocephalus go in two main directions. From the medical point of view, there is a need to find a better solutions for the diagnosis of disease activity. On the other hand, medical image processing deals mainly with challenging task of segmentation of brain ventricular system.

For many years the only indicator of hydrocephalus progress was Evan's ratio i.e. ratio between the transverse diameter of the anterior horns of the lateral ventricles to the greatest internal diameter of the skull [3]. CT brain scan with lines indicating diameters used for calculation of Evan's ratio is presented in Figure 1. Specifically, diameter A denotes anterior horns of the lateral ventricles and diameter B is the greatest internal diameter of the skull.

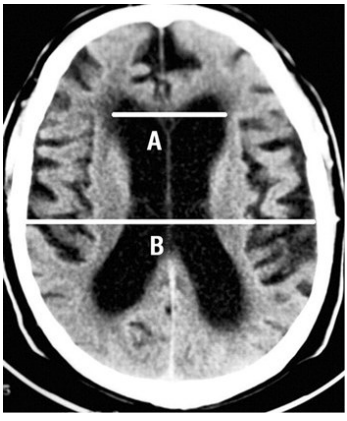

Fig. 1. CT brain scan lines indicating diameters used for calculation of Evan's ratio (A – anterior horns of the lateral ventricles, B – greatest internal diameter of the skull) [4]

International guidelines for the diagnosis of hydrocephalus indicate the active disease process when the Evan's ratio fluctuate above 0.3 [3]. However, current medical studies pay attention to inaccuracy of this method [1, 5]. It is believed that a better solution would be to calculate the volume of hydrocephalus directly from the volumetric CT brain scans [5, 9].

The calculation of ratio between the volume of the lesion to the volume of whole brain have been found to be more useful than Evan's approach and common linear measurements [6–8].

Today, ongoing research on medical image processing is only in a small extent involved with the problems of hydrocephalus. Challenging task of segmentation of the brain ventricular system has already been discussed [10–12]. However, methods for detection and quantitative assessment of the hydrocephalus are still under development and only several approaches have been reported [9, 13–14].

Research performed by Pustkova *et. al*. [9] was aimed at the segmentation and analysis of congenital hydrocephalus on a CT and MRI images. They calculated and compared the ventricular volumes from performed examinations before and after surgery, to find whether the treatment process was successful. However, this method works only for single images chosen manually by the radiologists and has a significant error in segmentation precision (up to 10%).

Butman and Linguraru [13] considered the problem of segmentation of postoperative communicating hydrocephalus. This disease is often recognized in patients with brain tumors. The method was based on combination of fast marching and geodesic active contour level sets. The main disadvantage of this technique is the computational overhead, which basically negates the possibility of applying the method in everyday clinical routine.

The objective of the research performed by Ambarki, *et al.* [14] was to test and evaluate the existing automatic tool for brain segmentation and analysis called Q_{brain}. They tested the application on 20 MRI datasets with indicated hydrocephalus. Q_{brain} can detect and calculate the volume of the hydrocephalus from the given images. Results of the research showed that this software can be used for comparison with existing measurement methods. However, Q_{brain} segmentation algorithm have some imperfections, so the calculated volume is often inaccurate.

Most of presented studies are generally new. This fact indicates the growing interest in that field. The main drawbacks of each of the abovementioned studies is that the segmentation results are often inaccurate and connected with the significant error in precision. Furthermore, the developed algorithms are often too complicated, which cause unacceptable computational overhead. For this reasons, it is significant to develop new segmentation methods for an automatic detection and assessment of the hydrocephalus. This is also the main problem regarded in this paper.

3. Input data

Images used in this paper are CT examinations. Several image data sets were tested. Every data set consisted of about 20 images of children brain. Each scan represented horizontal cross-section of the brain within a certain distance from the top of the patient head. Images had spatial resolution of 512×512 pixels, and were coded in 16-bit signed or unsigned short values.

Hydrocephalus is often clearly visible in CT images. This lesion can take two forms: (i) communicating, if there is a connection between all parts of the enlarged ventricular system and (ii) complex when one or more ventricular cysts are separated [3]. In both cases, the disease manifests itself as a dark (low intensity values) region in the image. Figure 2 shows a comparison between CT scan of a healthy brain (Fig. 2a) and brain affected by communicating form of hydrocephalus (Fig. 2b).

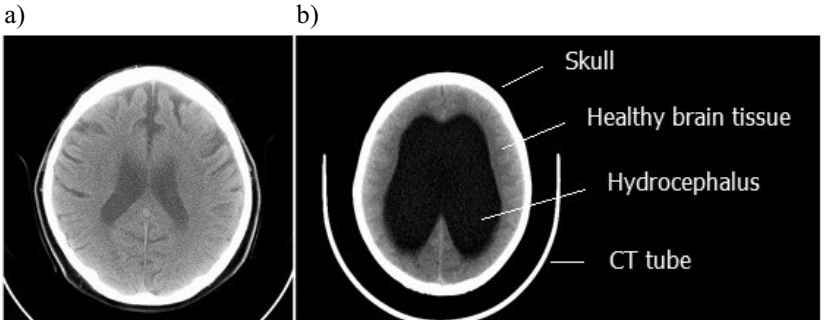

Fig. 2. Ventricular system of: (a) healthy brain and (b) brain affected by hydrocephalus

Recent CT scanners produce images in the international DICOM format. One of the most important features of this format is the information stored in the header of each file. DICOM header stores information of e.g. manufacturer name, the type of scan, image dimensions and pixel dependencies etc. For the purposes of this research, several parameters from DICOM header were particularly important. Table 1 shows variables from the DICOM header used in this research, with their short description.

Table 1
Selected parameters from DICOM header used in this work [15]

Variable code (group, element)	Variable name	Description
(0028,1052)	Rescale intercept	The value b in relationship between stored values (SV) and the output units. Output units = m*SV + b.
(0028,1053)	Rescale slope	The variable m in the equation specified by rescale intercept (0028,1052).
(0028,1050)	Window center	The variable describing the brightness of the image.
(0028,1051)	Window width	The variable describing the contrast of the image.

4. Methods and results

The aim of this research was to segment both: hydrocephalus and brain area from CT brain scans. For this purpose authors proposed image segmentation algorithms which can

be applied for precise detection of this disease. Such detection can be useful for further quantitative analysis of the key characteristic, like size of volume of the lesion.

Proposed methods may be the basis for further development of the system for an automatic detection and analysis of this lesion. Presented method was divided into three main stages:

- image preprocessing,
- brain segmentation,
- hydrocephalus segmentation.

4.1. Image preprocessing

In this step, each image from the input data set was normalized to a common intensity range. For brain segmentation pixel intensities were transformed to Hounsfield units[1] (range from –1024 to about 3071). According to the DICOM specification, every pixel in the image was scaled by the following formula:

$$g(x, y) = f(x, y) \cdot R_s + R_i \tag{1}$$

where:

$g(\cdot)$ – output pixel intensity,
$f(\cdot)$ – input pixel intensity,
R_s – rescale slope (see Tab. 1),
R_i – rescale intercept (see Tab. 1),
x, y – pixel coordinates.

After scaling image intensities, with the use of other DICOM header information, such as *Window width* and *Window center*, pixel intensities were transformed from signed to unsigned values without quality changes. The applied formula is given by Equation (2)

$$g'(x, y) = \begin{cases} g_{\min} \text{ for } g(x, y) \le a \\ g_{\max} \text{ for } g(x, y) > b \\ h(x, y) \text{ for } a < g(x, y) \le b \end{cases} \tag{2}$$

where:

$$a = c - 0.5 \cdot (2 - w) \tag{3}$$

$$b = c - 0.5 \cdot w \tag{4}$$

$$h(x, y) = \frac{g(x, y) - (c - 0.5)}{(w - 1) + 0.5} \cdot (g_{\max} - g_{\min}) + g_{\min} \tag{5}$$

[1] http://www.wikiradiography.com/page/Hounsfield++unit

$g'(\cdot)$ – input pixel intensity,
$g(\cdot)$ – output pixel intensity,
g_{min} – requested minimum output pixel intensity,
g_{max} – requested maximum output pixel intensity,
w – window width (see Tab. 1),
c – window center (see Tab. 1).

In case of CT images, 12 bits are sufficient to cover whole range of intensities. When using unsigned shorts, the data is shifted so all CT intensities become positive numbers in range from 0 to 4095 ($g_{min} = 0$, $g_{max} = 4095$). Figure 3 shows the result of preprocessing applied to exemplary image. Specifically, Figure 3a shows the input image and Figure 3b shows image after enhancement.

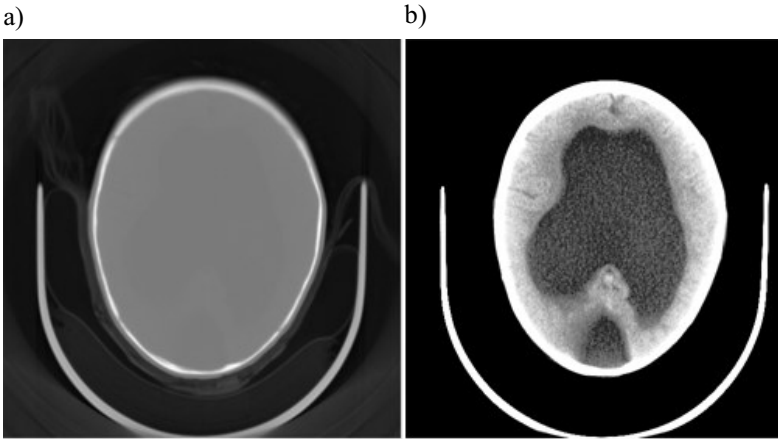

Fig. 3. Exemplary CT image before (a), and after (b) image enhancement

4.2. Brain segmentation

The second step was aimed at the extraction of the whole brain. This step is necessary for further quantitative assessment of the disease progress. Pixel transformation performed in the previous step significantly increased contrast of the image. As a result, the skull area together with the elements of the CT scanner tube could be easily removed by suppressing (setting to zero) any pixel in the image that is above 95% of the maximum pixel intensity value. Selected threshold was chosen empirically on the basis of observation of the distribution of pixel intensities after their transformation. Figure 4 shows the result of skull removal. Specifically, Figure 4a presents original image and Figure 4b shows image after preprocessing.

After removal of skull and CT tube, extraction of the whole brain area was possible. For this purpose, the 2D segmentation algorithm based on region growing was applied. This method requires the selection of initial seed point. It was decided to locate the seed at the center of the each cross-section as it is always contained in the brain area. The desired region originates from the exact location of this point. Then the region grows from the seed point to adjacent points depending on the selected threshold. Threshold value determines the scope of permissible difference of intensity between intensity of the candidate pixel and an average intensity of pixels already classified into the region. Figure 5 presents the overall schema of described algorithm.

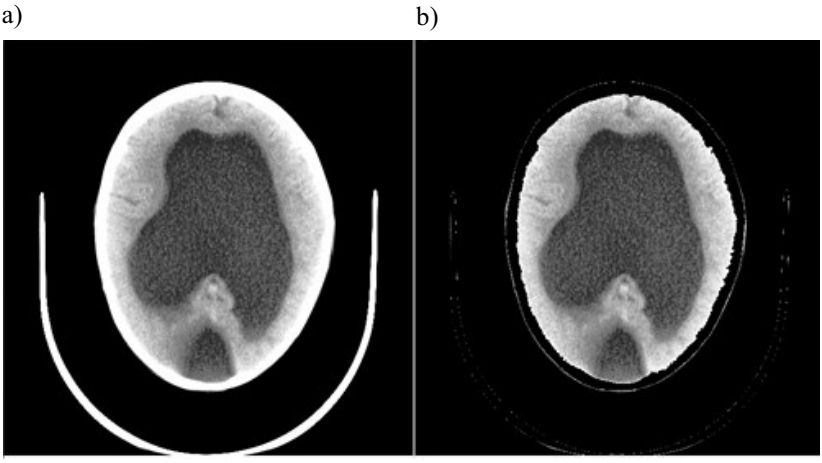

Fig. 4. Result of skull and CT tube removal: a) input image; b) image after preprocessing

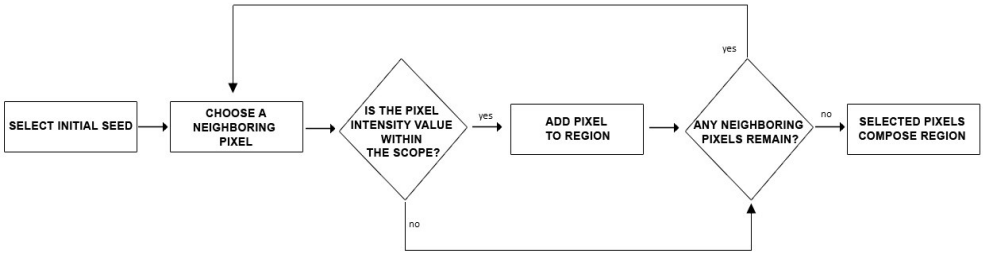

Fig. 5. Block diagram of developed segmentation algorithm based on region growing

Due to the almost complete separation of the skull from the whole brain area, the segmentation process is simple and effective. The final results of brain segmentation from several brain cross-sections are presented in Figure 6. Specifically, Figure 6a shows the original (input) images and Figure 6b shows images after brain segmentation.

a)

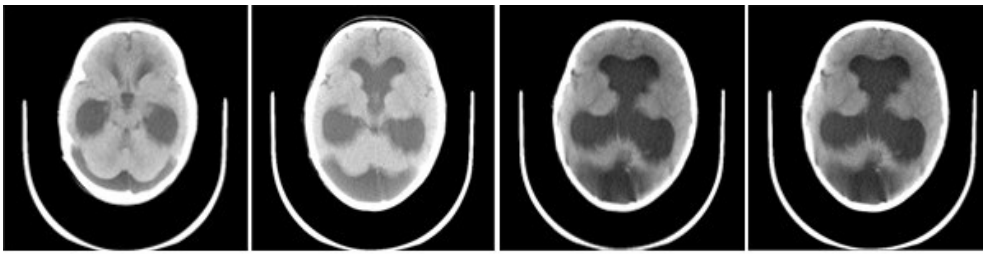

b)

Fig. 6. Result of brain extraction: a) original images; b) after brain segmentation

4.3. Hydrocephalus segmentation

Although hydrocephalus is clearly visible in the CT images, precise segmentation of this lesion is not a simple task. This is due to disruptions from diseases accompanied with hydrocephalus, such as edema or hematoma. Their intensities are very similar to intensities assigned to hydrocephalus.

It must be said that, in today's medical imaging, there is no clear criterion or common method to determine the precise area of the hydrocephalus. In addition, it's hard to find similar studies in the field of medical image processing, which were carried out already, hence achieved results can not be reliably compared. Therefore, the accuracy of the proposed segmentation algorithms can be assessed only in subjective way. For this reason, all of the presented methods and conclusions were consulted with specialists in the field of neurosurgery and radiology.

In our previous research, different segmentation algorithms were applied for hydrocephalus segmentation. Specifically, results of three popular thresholding algorithms were compared for analysis of results provided by the regarded thresholding methods (i.e. IsoData [16], Moments [17] and MaxEntropy [18]) the reader is referred to [19]. In this paper only results of 3D seeded region growing algorithm are presented. Obtained results were used for subjective verification of correctness of the 3D segmentation algorithm developed for the purposes of this research. Before main segmentation, median filter was applied to smooth contours of hydrocephalus. 3D segmentation algorithm, used in this step,

was similar to the one described in Section 4.2. The only change is that the user must manually indicate the seed point located inside the desired region. Starting from the indicated seed, the consecutive voxels are joined to the desired area. In this case, the threshold was also constant. The best results were obtained with the threshold value set at 0.3. Figure 7 presents results of 3D segmentation. The corresponding original images are shown in Figure 6a.

Fig. 7. Results of hydrocephalus segmentation using 3D region growing

Results of testing the developed 3D segmentation algorithm on several datasets shows that this algorithm gives subjectively better results than the traditional thresholding methods (see results in [19]). Due to the fact that this method has more potential for future development, this observation is considered satisfactory. However, the method in small extent is prone to leakages into areas not affected by the disease. This flaw occurs due to the side effects associated with hydrocephalus, that were mentioned earlier. Furthermore, it must be said that the leakage effect may often be caused by the low quality of the images from the datasets.

Segmentation results with indicated leakage effect may generate a mathematical error in further linear or volumetric measurements. The scope of the permissible error must be observed in medical practice and determined by the radiologists.

5. Conclusions

Paper presents results of applying image segmentation methods for the extraction of the brain area affected by the hydrocephalus. For this purpose, several thresholding algorithms were compared with the results of three-dimensional segmentation method based on region growing approach. For further quantitative assessment of the disease, the developed algorithm also involves obtaining the whole brain area.

Obtained results were positively reviewed by the specialists in the field of radiology and neurosurgery. Presented solution may be the basis for a system for an automatic detection and analysis of the hydrocephalus. Proposed methods are sufficient for an overall assessment of the progress of the disease. Obtained segmentation results allow to perform both linear (e.g. Evan's ratio) and volumetric measurements.

However, there are few requirements, when such measurements can be reliably compared. Firstly, the image datasets should be taken from the same device. Secondly, every examinations should be performed with the same settings of the device, number of taken images and position of the patient. Finally, the time difference between compared examinations should be low (ex. before and after surgery), because the children's brain is growing consequently.

The developed 3D segmentation algorithm based on region growing approach offers greater modification opportunities than traditional thresholding methods. Therefore, further research will be aimed at improving 3D segmentation algorithm by the development of pixel classification model combined with edge detection and interpolation. Accurate segmentation results will be used to calculate the approximate volume of the lesion and the volume of the whole brain by counting the number of pixels classified to each considered area. Such calculations can be compared and verified with measurements taken with commonly used linear assessment methods.

Acknowledgements

The authors would like to thank the Department of Neurosurgery of Polish Mother's Memorial Hospital – Research Institute in Lodz for providing the CT datasets used in this research.

Tomasz Węgliński is a scholarship holder of project entitled "Innovative education ..." supported by European Social Fund.

Anna Fabijańska receives financial support from the Foundation for Polish Science in a framework of START fellowship and from Ministry of Science and Higher Education of Poland in a framework of research project no. N N516 490439 (funds for science in years 2010–2012).

References

[1] Zakrzewski K., *Wodogłowie i inne zaburzenia krążenia płynu mózgowo-rdzeniowego u dzieci*. Czelej, Lublin 2007 (in Polish).

[2] Zakrzewski K., Polis L., *Wodogłowie u dzieci*. Print-Pol, Łódź 1999 (in Polish).

[3] Factora R., *When do common symptoms indicate normal pressure hydrocephalus?* Cleveland Clinic Journal of Medicine, vol. 73, No. 5, 2006, 447–450.

[4] Malm J., Eklund A., *Idiopathic normal pressure hydrocephalus*. Practical Neurology, vol. 6, 2006, 14–27.

[5] Ambarki K., Israelsson H., Wahlin A., Birgander R., Eklund A., Malm J., *Brain ventricular size in healthy elderly: comparison between Evans index and volume measurement*. Neurosurgery, vol. 67, No. 1, 2010, 94–99.

[6] Bradleya W.G., Safara F.G., Hurtadoa C., Orda J., Alksneb J.F., *Increased intracranial volume: A clue to the etiology of idiopathic normal-pressure hydrocephalus?* American Journal of Neuroradiology, vol. 25, No. 9, 2004, 1479–1484.

[7] Tsunoda A., Mitsuoka H., Bandai H., Arai H., Sato K., Makita J., *Intracranial cerebrospinal fluid distribution and its postoperative changes in normal pressure hydrocephalus*. Acta Neurochir, vol. 143, No. 5, 2001, 493–499.

[8] Toma A.K., Holl E., Kitchen N.D., Watkins L.D., *Evans' index revisited: The need for an alternative in normal pressure hydrocephalus*. Neurosurgery, vol. 68, No. 4, 2011, 939–944.

[9] Pustkova R., Kutalek F., Penhaker M., Novak V., *Measurement and calculation of cerebrospinal fluid in proportion to the skull*. 9th RoEduNet IEEE International Conference, RoEduNet, Romania, 2010, 95–99.

[10] Liu J., Huang S., Nowinski W.L., *Automatic segmentation of the human brain ventricles from MR images by knowledge-based region growing and trimming*. Neuroinformatics, vol. 7, No. 2, 2009, 131–146.

[11] Schnack H.G., Hulshoff Pol H.E., Baaré W.F.C., Viergever M.A., Kahn R.S.: *Automatic segmentation of the ventricular system from MR images of the human brain*. NeuroImage, vol. 14, No. 1, 2001, 95–104.

[12] Hatfield F.N., Dehmeshki J., *Automatic delineation and 3-D visualisation of the human ventricular system using probabilistic neural networks.* Proc. of SPIE – The International Society for Optical Engineering, No. 3409, 1998, 361–367.

[13] Butman J.A., Linguraru M.G., *Assessment of ventricle volume from serial MRI scans in communicating hydrocephalus*. 5th IEEE International Symposium on Biomedical Imaging: From Nano to Macro, 2008, 49–52.

[14] Ambarki K., Wahlin A., Birgander R., *et al*., *MR imaging of brain volumes: Evaluation of a fully automatic software.* American Journal of Neuroradiology, vol. 32, No. 2, 2011, 408–412.

[15] http://medical.nema.org/dicom/2004.html, *Digital Imaging and Communications in Medicine*, retrieved in April 2011.

[16] Ridler T.W., Calvard S., *Picture thresholding using an iterative selection method.* IEEE Transactions on Systems, Man and Cybernetics SMC-8, vol. 8, 1978, 630–632.

[17] Tsai W.-H., *Moment-preserving thresholding: a new approach*. Computer Vision, Graphics & Image Processing, vol. 29, No. 3, 1985, 377–393.

[18] Kapur J.N., Sahoo P.K., Wong A.K.C., *A new method for gray-level picture thresholding using the entropy of the histogram*. Computer Vision, Graphics, & Image Processing, vol. 29, No. 3, 1985, 273–285.

[19] Węgliński T., Fabijańska A., *The concept of image processing algorithms for assessment and diagnosis of hydrocephalus in children*. 2nd International Interdisciplinary Ph.D. Workshop, 2011 (in print).